NJC

Accepted Manuscript

This article can be cited before page numbers have been issued, to do this please use: J. Zhao, Y. Leng, P. Jiang, J. Wang and C. Zhang, *New J. Chem.*, 2015, DOI: 10.1039/C5NJ01541C.

Cite this: DOI: 10.1039/c0xx00000x

www.rsc.org/xxxxxx

ARTICLE TYPE

POSS-Derived Mesoporous Ionic Copolymer-Polyoxometalate Catalysts with Surfactant Function for Epoxidation Reactions

Jiwei Zhao,[a] Yan Leng,*[a] Pingping Jiang,[a] Jun Wang[b], and Chenjun Zhang [a]

Received (in XXX, XXX) XthXXXXXXXXX 20XX, Accepted Xth XXXXXXXXX 20XX
DOI: 10.1039/b000000x

A series of novel polyoxometalate (POM)-based stable polymeric hybrids were successfully synthesized using polyhedral oligomeric vinylsilsesquioxanes (POSS) and ionic liquids (IL) bearing hydrophobic alkyl chains as the building blocks, followed by ion exchange with Keggin-type phosphotungstic acid (PW). The obtained hybrids POSS-IL*x*-PW were demonstrated to be mesostructured and amphiphilic materials with good thermal stability. Catalytic tests for H_2O_2-based epoxidation of cyclooctene have shown that these newly designed catalysts exhibit extraordinary catalytic activities, catalytic rate, and quite stable reusability. The unique amphiphilic property and the mesoporous structure are revealed to be responsible for the catalysts' excellent performance in epoxidation reactions with H_2O_2.

1. Introduction

Polyoxometalates (POMs) is a class of transition-metal oxygen anion clusters with structural versatility [1,2]. Owing to their well-defined physical and chemical properties and reversible electron transformation abilities, POMs have been extensively investigated as catalysts in a variety of oxidation reactions, including epoxidation of alkenes [3-6]. However, their rich redox properties are strongly hindered by good solubility in common polar solvents and hydrophilcity, which causes difficulty in separation and recycling of the catalysts. To overcome this obstacle, a numbers of strategies have been developed for the heterogenisation of POM catalysts, including phase transformation, microemulsion formation, encapsulation by inorganic or organic cations, and immobilization into polymer or silica matrix [7-10]. In this context, assembling of POMs with polymeric organic cations is revealed to be a successful example for preparing heterogeneous POM catalysts, which is beneficial for adjusting the solubility, redox properties, and surface microenvironment of POM. For example, Doherty [11] prepared a POM-based linear cation-decorated polymeric hybrid and used it as an efficient and recyclable catalyst for the epoxidation of allylic alcohols and alkenes. We have prepared a series of POM-based polymeric ionic hybrids by combining poly(ionic liquid) cations which heteropolyanions, and the resulting ionic solids turned out to be effective catalysts for acid-catalyzed or oxidative organic transformations [12-16]. Nevertheless, the self-assembled POM polymeric hybrids are always nonporous, and limited the heterogeneous catalytic activity in mass-transfer-controlled systems [17,18]. Moreover, the hydrophilic or hydrophobic frameworks of polymeric cations may hinder the interaction of the POM catalytic centers with the hydrophobic organic substrates or hydrophilic oxidizing agent H_2O_2, which results in limited catalytic efficiency. Therefore, a rationally designed mesoporous POM-based polymeric catalysts with optimized amphipathicity is needed.

Polyhedral oligomeric silsesquioxanes (POSS) are recently regarded as ideal building blocks for constructing organic-inorganic hybrid materials [19,20]. POSS is a class of typical organic-inorganic molecules with the general formula $R_8Si_8O_{12}$, where R is hydrogen or organic groups, such as alkyl, aryl or any of their derivatives. They have unique star-shaped nanostructures and chemical properties, such as facile chemical modification, good pH tolerance, high temperature and oxidation resistance properties [21-23]. So far, micro/mesoporous materials based on POSS precursors have been prepared by various chemical routes including hydrosilation methods, thermolysis, and copper-mediated coupling [24-27]. However, there are little reports on the preparation of POSS-derived micro/mesoporous poly(ionic liquid) materials for catalysis.

Very recently, we have synthesized a series of POSS-containing porous ionic polymer materials for epoxidation reactions, but the pore size distribution of these materials is too wide [28,29]. Herein, we demonstrate a successful preparation of mesoporous POM-based polymeric hybrids by copolymerization of octavinyl POSS with IL monomers without using any templates, followed by ion exchange with the Keggin-type $H_3PW_{12}O_{40}$. With the concept of adjusting of interfacial microenvironment of POM catalysts in mind, a series of imidazole IL bearing hydrophobic alkyl chains with different lengths were synthesized and introduced into the polymeric hybrids. The catalysts not only exhibit enhanced catalytic activities for the epoxidation of alkenes using H_2O_2 but also provide easy catalyst recovery from the reaction system. The excellent catalytic performance of the catalysts is mostly attributed to the contributions of the mesoporous structure and the amphiphilic interfacial microenvironment of the catalysts.

View Article Online
DOI: 10.1039/C5NJ01541C

2. Experimental section

2.1 Materials and methods

All chemicals were analytical grade and used as received. ^{1}H-NMR spectra were measured with a Bruker DPX 300 spectrometer at ambient temperature in D_2O or $CDCl_3$ using TMS as internal reference. FT-IR spectra were recorded on a Nicolet 360 FT-IR instrument (KBr discs) in the 4,000-400 cm^{-1} region. TG analysis was carried out with a STA409 instrument in dry air at a heating rate of 10 ℃/min. SEM image was performed on a HITACHI S-4800 field-emission scanning electron microscope. TEM images were obtained with JEOL JEM-2100 electron microscope operated at 200 Kv. The pore size distribution was derived from the desorption branch of N_2 isotherms using Barrett-Joyner-Halenda (BJH) method. Electrospray ionization mass spectra (ESI-MS) were recorded with a Finnigan mat APISSQ 710 mass spectrometer.

2.2 Catalyst preparation

2.2.1 Preparation of IL monomers

Typically, [3-octyl-1-vinylimidazolium]Br (OIM) was prepared as follows: N-vinylimidazole (4.71 g, 50 mmol) and 1-bromooctane (9.66 g, 50 mmol) were dissolved in ethanol (25 mL) at 80°C for 48 h under nitrogen atmosphere with stirring. On completion, the solvent was removed by reduced pressure distillation, the remained liquid mixture was washed with anhydrous diethyl ether for three times, and then dried in vacuum at 50 ℃ for 12 h to give the IL product OIM. ^{1}H NMR (300 MHz, $CDCl_3$, TMS) δ (ppm) =0.72 (s, 3H, $-CH_3$), 1.13 (m, 10H, $-CH_2$), 1.78 (m, 2H, $-CH_2$), 3.51 (m, 2H, $-CH_2$), 5.25 (d, 1H, -CH), 5.95 (d, 2H, $-CH_2$), 7.32 (d, 2H, -CH), 7.62 (d, 1H, -CH) (Figure S2 in Supporting Information (SI)). The ILs [3-butyl-1-vinylimidazolium]Br (BIM), [3-dodecyl-1-vinylimidazolium]Br (DIM), and [3-hexadecyl-1-vinylimidazolium]Br (HIM) were prepared in the same way. ^{1}H NMR (300 MHz, $CDCl_3$, TMS) for BIM: δ (ppm) =0.94 (t, 3H, $-CH_3$), 1.35 (m, 2H, $-CH_2$), 1.92 (m, 2H, $-CH_2$), 3.68 (m, 2H, $-CH_2$), 5.36 (d, 1H, -CH), 6.01 (d, 2H, $-CH_2$), 7.27 (d, 2H, -CH), 7.67 (d, 1H, -CH) (Figure S1 in SI). ^{1}H NMR (300 MHz, $CDCl_3$, TMS) for DIM: δ (ppm) =0.9 (s, 3H, $-CH_3$), 1.3 (m, 18H, $-CH_2$), 1.97 (m, 2H, $-CH_2$), 3.74 (m, 2H, $-CH_2$), 5.43 (d, 1H, -CH), 5.93 (d, 2H, $-CH_2$), 7.33 (d, 2H, -CH), 7.60 (d, 1H, -CH) (Figure S3 in SI). ^{1}H NMR (300 MHz, $CDCl_3$, TMS) for HIM: δ (ppm) =0.83 (t, 3H, $-CH_3$), 1.27 (m, 26H, $-CH_2$), 1.93 (m, 2H, $-CH_2$), 3.67 (m, 2H, $-CH_2$), 5.38 (d, 1H, -CH), 6.01 (d, 2H, $-CH_2$), 7.26 (d, 2H, -CH), 7.54 (d, 1H, -CH) (Figure S4 in SI). The ^{1}H NMR spectra are shown in the Supporting Information (SI) Figures S1-S4. Positive-ion electrospray ionization mass spectrometry (ESI-MS) *m/z*: 151.1 [3-butyl-1-vinylimidazolium]$^+$ (Figure S5A in SI), 207.5 [3-octyl-1-vinylimidazolium]$^+$ (Figure S6A in SI), 264.2 [3-dodecyl-1-vinylimidazolium]$^+$ (Figure S7A in SI), and 320 [3-hexadecyl-1-vinylimidazolium]$^+$ (Figure S8A in SI). Negative-ion electrospray ionization mass spectra show the patterns at 79 and 81 (Br^-) (Figures S5B-S8B).

2.2.2 Preparation of octavinyl POSS

Octavinyl POSS was prepared according to the previous literature [30,31]. Typically, in a 250 mL flask, vinyltriethoxysilane (19 g, 0.1 mol) was dissolved in 50 mL anhydrous ethanol. Then 10 mL hydrochloric acid and 8 mL deionized water were added into the above solution with vigorous stirring. The above reaction mixture was allowed to react for 48 h at room temperature. On completion, the white crystalline powder was filtered, washed with anhydrous ethanol, recrystallized in tetrahydrofuran/methanol (volume ratio: 1:3) and dried in vacuum at 80 ℃ for 10 h. ^{29}Si NMR (400 MHz, $CDCl_3$, TMS) δ (ppm) = 80.19 (Figure S9 in SI).

2.2.3 Preparation of POSS-ILs

POSS-IL$_x$ (*x* stands for the molar ratio of IL to POSS) were synthesized through free radical polymerization of octavinyl POSS and IL. As a typical run for the synthesis of POSS-OIM$_8$, the obtained octavinyl POSS (0.63 g, 1 mmol), OIM (2.30 g, 8 mmol), and azodiisobutyronitrile (AIBN, 0.06 g) were dissolved in a mixture solvent (1,4-dioxane 20 mL and ethanol 20 mL). Then the solution was stirred at 75^{o}C for 24 h. After reaction, the above mixture was added dropwise into ethyl acetate (100 mL) to afford the solid product. Then the solid product POSS-OIM$_8$ was filtered, washed with ethanol and dried under vacuum. The ionic polymers POSS-OIM$_4$, POSS-OIM$_{12}$, POSS-OIM$_{16}$, POSS-BIM$_8$, POSS-DIM$_8$, and POSS-HIM$_8$ were prepared accordingly.

2.2.4 Preparation of POSS-ILs-PW

Polymeric hybrids POSS-IL$_x$-PW were prepared from the reaction between POSS-IL$_x$ and $H_3PW_{12}O_{40}$ (PW). For example, the starting molar ratio of POSS-OIM$_x$ to PW was 1:(*x*/3). Typically, POSS-OIM$_x$ and PW were dissolved in anhydrous

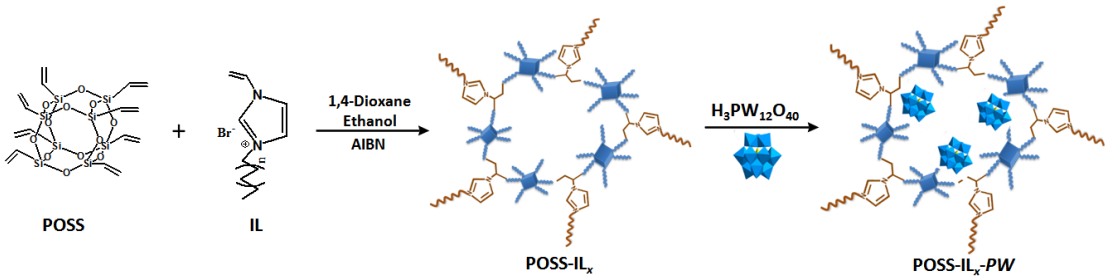

Figure 1. Figure 1. Schematic preparation of the POSS-derived mesoporous catalysts.

View Article Online
DOI: 10.1039/C5NJ01541C

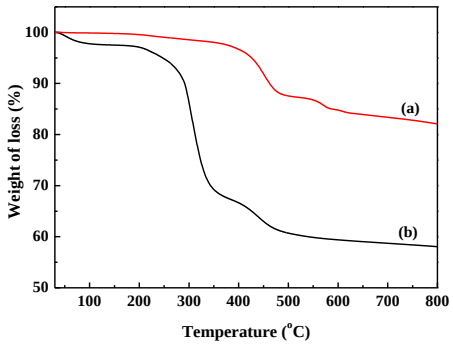

Figure 2. TG curves of (a) POSS-OIM$_8$-PW and (b) POSS-OIM$_8$.

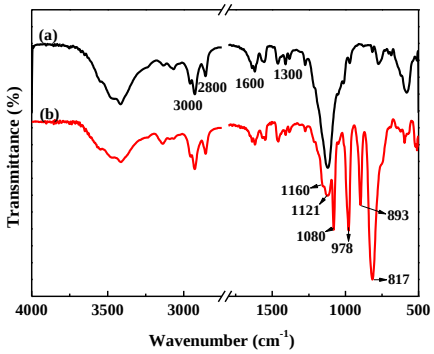

Figure 3. FTIR spectra of (a) POSS-OIM$_8$ and (b) POSS-OIM$_8$-PW.

ethanol (20 mL) and deionized water (20 mL), respectively. Then the aqueous solution of PW was added into the POSS-OIM$_x$ solution, followed by stirring at room temperature for 2 h. The solid product POSS-OIM$_8$-PW was filtered, washed with deionized water and ethanol, and dried. The polymeric hybrids POSS-BIM$_8$-PW, POSS-DIM$_8$-PW and POSS-HIM$_8$-PW were prepared accordingly.

2.3 Catalytic tests

Cyclooctene (10 mmol), acetonitrile (10 mL), and catalyst (0.1 g, 0.025 mmol) were added into a 25 mL flask. Then 30 wt.% H_2O_2 (12 mmol) was added into the solution at 70°C within 10 min under vigorous stirring. After reaction, the reaction mixture was centrifuged to remove the solid catalyst, and the liquid was analyzed by a gas chromatography (GC). Other alkene substrates were tested accordingly. A five-run catalyst recycling was carried out for testing the reusability of catalyst.

3. Results and discussion

3.1 Catalyst preparation and characterization

The preparation of the POM-paired polymeric hybrids was carried out according to the procedures shown in Figure 1. Typically, the IL monomer OIM was first prepared and characterized by ^{1}H NMR. The POSS-containing ionic copolymer was synthesized by the free radical copolymerization of octavinyl POSS and OIM using AIBN as the initiator. By varying the molar ratio of OIM to POSS and the types of alkyl side chain in imidazole IL, a series of ionic copolymers POSS-IL$_x$ could be prepared in the same way. The final catalysts POSS-OIM$_x$-PW

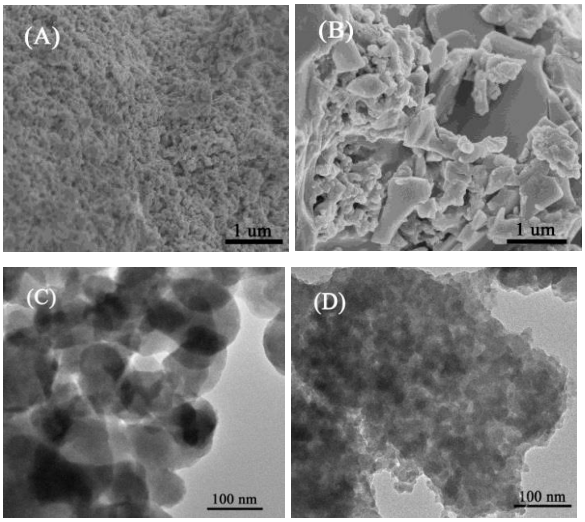

Figure 4. SEM images of (A) POSS-OIM$_8$-PW and (B) OIM-PW, and TEM images of (C) POSS-OIM$_8$ and (D) POSS-OIM$_8$-PW.

were obtained by the anion-exchange of POSS-OIM$_x$ with $H_3PW_{12}O_{40}$ in aqueous solution. The TG profile of POSS-OIM$_8$ shows that the small weight loss of 2-3% around 100-110 ℃ results from the loss of the adsorbed water. However, POSS-OIM$_8$-PW is quite stable up to ca. 400 °C. The weight loss of nearly 38% and 70% for POSS-OIM$_8$-PW and POSS-OIM$_8$, respectively, are attributed to the decomposition of organic groups. Thus, the content of PW on the POSS-OIM$_8$-PW was calculated to be 45.7%, suggesting a high PW loading capacity of POSS-OIM$_8$.

Figure 3 illustrates the FT-IR spectra of the prepared samples POSS-OIM$_8$-PW and POSS-OIM$_8$. The FT-IR spectrum of POSS-OIM$_8$ clearly shows the strong band at 1121 cm^{-1} assigned to asymmetric vibration of Si-O-Si and the characteristic bands at 1300~1600 cm^{-1} and 2800~3000 cm^{-1} that are assigned to organic groups, indicating the coexistence of POSS and IL units. After the combination of POSS-OIM$_8$ with $H_3PW_{12}O_{40}$, the characteristic vibration bands for the $[PW_{12}O_{40}]^{3-}$ species are observed at 1080, 978, 893 and 817 cm^{-1}, assignable to vibrations of P–O$_a$, W=O$_d$, W–O$_b$–W and W–O$_c$–W, respectively [32-35]. Moreover, the position of the peaks assigned to POSS and organic moiety in POSS-OIM$_8$-PW are well consistent with those of the IR spectrum for POSS-OIM$_8$.

Figure 4 illustrates the SEM images of POSS-OIM$_8$-PW and OIM-PW. It is demonstrated that the POSS-OIM$_8$-PW (Figure 4A) have irregular honeycomb-shaped morphology with micrometer size and nanoscale hollow structure. In the case of POSS-free hybrid OIM-PW (Figure 4B), the morphology changed to angular blocks with a smooth surface. In the TEM image of POSS-OIM$_8$, the black micelles with size of 15-20 nm are clearly seen, demonstrating the existence of POSS unites (Figure 4C). The black portion was obviously increased in the TEM image of POSS-OIM$_8$-PW (Figure 4D), which indicates that the introduced PW has been uniformly dispersed in the copolymer network.

The surface area and pore structure of POSS-OIM$_8$-PW was examined by nitrogen sorption measurements. As shown in Figure 5A, the isotherm of POSS-OIM$_8$-PW is IV type with a clear H1-type hysteresis loop at a relatively higher partial

View Article Online
DOI: 10.1039/C5NJ01541C

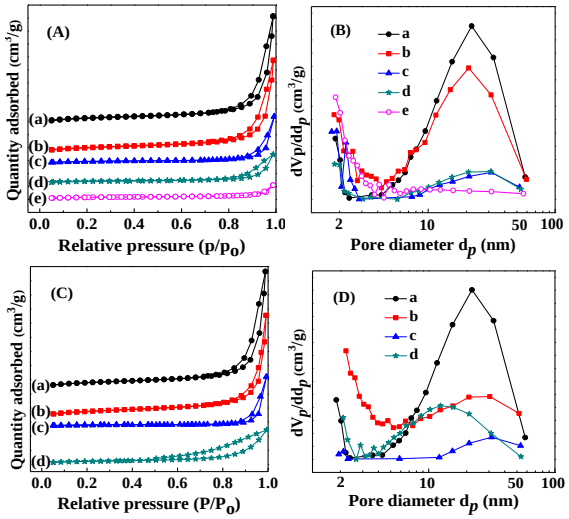

Figure 5. (A) Nitrogen adsorption–desorption isotherms and (B) BJH pore size distributions of (a) POSS-OIM$_8$-PW, (b) POSS-OIM$_{12}$-PW, (c) POSS-OIM$_{16}$-PW, (d) POSS-OIM$_4$-PW, (e) OIM-PW, and (C) Nitrogen adsorption–desorption isotherms and (D) BJH pore size distributions of (a) POSS-OIM$_8$-PW, (b) POSS-DIM$_8$-PW, (c) POSS-HIM$_8$-PW, (d) POSS-BIM$_8$-PW.

Table 1. The textural parameters of various samples.

Entry	Catalyst	S_{BET}[a] ($m^2 g^{-1}$)	V_p[b] ($cm^3 g^{-1}$)	D_v[c] (nm)
1	OIM-PW	2.1	0.006	11.0
2	POSS-OIM$_4$-PW	7.1	0.057	32.4
3	POSS-OIM$_8$-PW	25.0	0.175	22.0
4	POSS-OIM$_{12}$-PW	18.7	0.129	21.6
5	POSS-OIM$_{16}$-PW	12.7	0.099	30.3
6	POSS-BIM$_8$-PW	8.2	0.038	11.5
7	POSS-DIM$_8$-PW	18.6	0.122	24.2
8	POSS-HIM$_8$-PW	5.9	0.037	18.4

[a] BET surface area, [b]Total pore volume, [c]Average pore size.

pressure region of P/P_0 = 0.8−1.0, indicating the presence of mesoporosity. The BET surface area and the total pore volume are 25.0 m^2/g and 0.175 cm^3/g, respectively (Table 1, entry 3). The most probable distribution in mesopores appears at 22.0 nm. However, the POSS-free polymeric hybrid OIM-PW is a nonporous material, with a surface area of only 3.4 m^2/g (Table 1, entry 1). These results demonstrate that the POSS plays important roles in the formation of mesotructures. The primary result encouraged us to prepare and test a series of catalysts POSS-OIM$_x$-PW with different molar ratio of OIM to POSS, with the nitrogen sorption isotherms and pore size distribution curves for the resultant samples displayed in Fig 5(A) and (B), respectively. Clearly, all the samples POSS-OIM$_4$-PW, POSS-OIM$_{12}$-PW, and POSS-OIM$_{16}$-PW give typical type-IV isotherms at the pressure of 0.8< P/P_0<1 and relative wide pore size distribution curves with the most probable pore sizes of 25-35 nm (Table 1, entries 2-5), reflecting a typical mesostructure. However, the low content or high content of POSS tends to give less porous systems and causes continuous decline in BET surface areas and pore sizes.

Table 2. Catalytic performances of various catalysts for epoxidation of cyclooctene with H_2O_2[a].

Entry	Catalyst	Solubility in reaction	Con[b] (%)	Sel[c] (%)
1	-	Homogeneous	-	-
2	$H_3PW_{12}O_{40}$	Homogeneous	11	85
3	POSS-OIM$_8$	Heterogeneous	1.3	37
4	POSS-OIM$_4$-PW	Heterogeneous	81	>99
5	POSS-OIM$_8$-PW	Heterogeneous	>99	>99
6	POSS-OIM$_{12}$-PW	Heterogeneous	>99	>99
7	POSS-OIM$_{16}$-PW	Heterogeneous	97	>99
8	POSS-BIM$_8$-PW	Heterogeneous	90	>99
9	POSS-DIM$_8$-PW	Heterogeneous	99	>99
10	POSS-HIM$_8$-PW	Heterogeneous	98	>99
11	BIM-PW	Heterogeneous	45	>99
12	OIM-PW	Heterogeneous	52	98
13	DIM-PW	Heterogeneous	77	98
14	HIM-PW	Heterogeneous	80	98

[a] Reaction conditions: catalyst (0.03 mmol), cyclooctene (10 mmol), 30% H_2O_2 (12 mmol), acetonitrile (10 mL), 70°C, 2 h. [b] Conversion of cyclooctene. [c] Selectivity for the epoxide product.

For example, when the molar ratio of OIM to POSS is 16:1, the BET surface area and the pore volume are 12.7 m^2/g and 0.099 cm^3/g, respectively, and when the molar ratio of OIM to POSS is 4:1, the BET surface area and the pore volume are only 7.1 m^2/g and 0.051 cm^3/g, respectively. Therefore, the surface area and pore structure can be adjusted flexibly through turning the POSS content. These results further confirm that the POSS is significant for the pore formation. With POSS and ILs at molar ratio of 1:8, we further studied the effect of ILs bearing different length of alkyl chains on the pore structure. As can be seen in Firgure 5C and 5D, although all the samples show typical type-IV isotherms, giving a steep increase at a pressure of 0.8< P/P_0<1, the rather short length or long length of alkyl chains led to low BET surface areas (less than 10 m^2/g), pore volumes, and the most probable pore sizes. This is probably due to that the ILs bearing short alky chain is difficult to form micelle during the catalyst preparation process, which is not beneficial for the formation of porous structure, and the ILs bearing long alky chain may block up the already formed channel of the final catalyst. Therefore, the optimum specific surface 25.0 m^2/g and pore volume 0.175 cm^3/g were obtained when the mole ratio of POSS to OIM was 1:8.

3.2 Catalytic activity in the epoxidation reaction

The catalytic performances of various catalysts were assessed in the epoxidation of the probe substrate cyclooctene with aqueous H_2O_2 as oxidant and acetonitrile as solvent, and the

View Article Online
DOI: 10.1039/C5NJ01541C

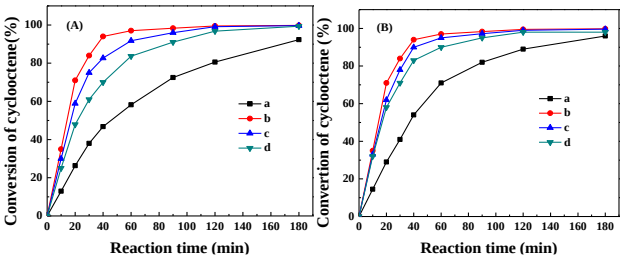

Figure 6. (A) Catalytic kinetics of (a) POSS-OIM$_4$-PW, (b) POSS-OIM$_8$-PW, (c) POSS-OIM$_{12}$-PW, (d) POSS-OIM$_{16}$-PW, and (B) catalytic kinetics of (a) POSS-BIM$_8$-PW, (b) POSS-OIM$_8$-PW, (c) POSS-DIM$_8$-PW, (d) POSS-HIM$_8$-PW.

Table 3. Epoxidation of various alkenes with H_2O_2 catalyzed by POSS-OIM$_8$-PW[a].

Entry	Substrate	Reaction time (h)	Con[b] (%)	Sel[c] (%)
1[d]	Cyclooctene	2	100/100/99/99/99	100
2	Cyclohexene	4	93	94
3	1-octene	6	51	99
4	1-hexene	6	57	95
5	Bipentene	3	81	83
6	Cis-3-hexenol	4	90	97
7	Styrene	6	72	66

[a] Reaction conditions: catalyst (0.03 mmol), substrates (10 mmol), 30% H_2O_2 (12 mmol), acetonitrile (10 mL), 70°C. [b] Conversion of cyclooctene. [c] Selectivity for the epoxide product. [d] Five-run recycling test. Byproducts for entry 2: 2-cyclohexen-1-ol ; entry 3: octylaldehyde; entry 4: 2-hexenone; entry 5: 3,4-epoxyhexane-1-aldehyde; entry 6: 1,2-ene-*p*-menth-8,9-epoxy; entry 7: benzaldehyde.

results are summarized in Table 2. In the absence of catalyst, the reaction did not proceed at all (entry 1). The POSS-OIM$_8$ and pure $H_3PW_{12}O_{40}$ display very low activities and poor selectivity (entries 2 and 3). We were glad to find that the newly synthesized mesoporous catalyst POSS-OIM$_8$-PW caused a heterogeneous catalysis, and exhibit very high conversion of 99% with 100% selectivity (entry 5). Other mesoporous samples POSS-OIM$_x$-PW with different molar ratio of OIM to POSS also show excellent activities (> 95%) (entries 6 and 7), with the exception of POSS-OIM$_4$-PW that offer a 81% conversion (entry 4), but it is still much higher than that of POSS-free nonporous sample OIM-PW, which shows a 52% conversion with 98% selectivity (entry 11). The above results suggest that the excellent performance of POSS-OIM$_x$-PW may be relates to the mesoporous structure. For the catalysts POSS-IL$_8$-PW containing different IL, POSS-BIM$_8$-PW having a C4 hydrophobic tail displays a 90% conversion (entry 8), which is lower than those of the catalysts POSS-OIM$_8$-PW, POSS-DIM$_8$-PW and POSS-HIM$_8$-PW carrying C8, C12, and C16 alkyl chain, respectively (entries 5, 9 and 10). Also notably, for the POSS-free samples containing different IL, the increase of the length of alkyl chain in IL leads to continuous increase in the catalytic conversion from 45% to 80% (entries 11-14). However, they are much lower than those of the POSS-containing ones. The above special comparisons further indicate

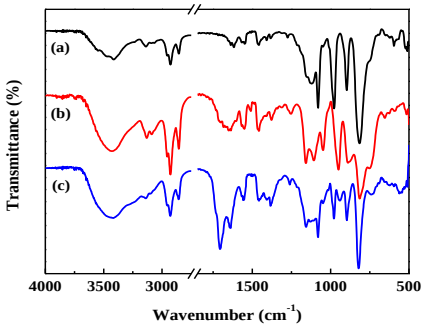

Figure 7. FT-IR spectra of (a) fresh POSS-OIM$_8$-PW, (b) two recycled POSS-OIM$_8$-PW, and (c) five recycled POSS-OIM$_8$-PW.

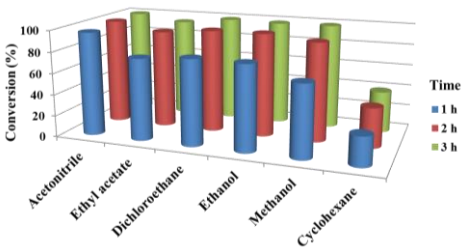

Figure 8. Catalytic activities of POSS-OIM$_8$-PW in epoxidation of cyclooctene with H_2O_2 in different solvents.[a]
[a] Reaction conditions: catalyst (0.03 mmol), cyclooctene (10 mmol), 30% H_2O_2 (12 mmol), solvent (10 mL), 70°C.

that the POSS units are indispensable for the high activities of the target PW catalyst for epoxidation of cyclooctene with H_2O_2. Moreover, the polymer hybrid catalysts bearing hydrophobic tails of different lengths might supply a different microenvironment on the surface of the catalyst for the reactions and strongly affect the catalytic activity.

The results in Table 2 demonstrate that most of the catalysts POSS-IL$_x$-PW could catalyze the epoxidation of cyclooctene with H_2O_2 in the reaction time of 2 h, giving satisfactory activities and selectivity. However, during the reaction process, we found that the catalytic reaction rate of POSS-IL$_x$-PW has the obvious difference. Thus, we tested the catalytic kinetics of POSS-IL$_x$-PW for the epoxidation of cyclooctene in acetonitrile solvent. The results are illustrated in Figure 6A and 6B. For all these catalysts, the increase of the reaction time led to a smoothly increase in the cyclooctene conversion, the maximum conversions were achieved at the reaction time of 3 h. Among which, POSS-OIM$_8$-PW exhibits the fast reaction rate, the conversion reached nearly 90% at the reaction time of only 30 min, and the reaction can be completed within 1 h.

Encouraged by the above results, other alkene substrates such as cyclohexene, 1-octene, 1-hexenel, bipentene, cis-3-hexeno and styrene were also investigated on the catalyst POSS-OIM$_8$-PW, with the results list in Table 3. It can be seen that the present catalyst POSS-OIM$_8$-PW could be applied to the epoxidation of various alkenes using H_2O_2, and optimum results of activities and selectivity were obtained as well. To assess catalytic reusability POSS-OIM$_8$-PW was recovered simply by filtration and then reused for the next run without adding any fresh catalyst. Table 3 entry 1 displays the result of the five-run recycling test of POSS-OIM$_8$-PW for the epoxidation of cyclooctene. There is no

View Article Online
DOI: 10.1039/C5NJ01541C

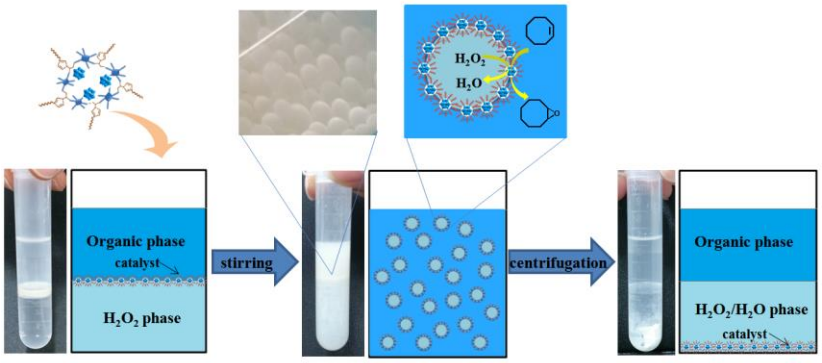

Figure 9. Possible mechanism for biphasic epoxidation of alkenes over amphiphilic catalysts.

decrease in the conversion is observed in the recycling runs, implying good potential for catalyst reuse. Further, the IR spectra of the recycled catalysts (Figure 7) are well consistent with that of the fresh one, revealing a durable catalyst structure.

Figure 8 shows the catalytic performances of POSS-OIM$_8$-PW in the epoxidation of cyclooctene with H_2O_2 in different solvents over the reaction times of 1 h, 2 h, and 3 h, respectively. During the reaction process, the catalyst POSS-OIM$_8$-PW was insoluble in all cases, and exhibited different catalytic activities with satisfying selectivity above 99%. In the acetonitrile, ethanol, and methanol solvent, liquid-solid heterogeneous catalysis system was observed, and excellent conversions were obtained after the reaction time of 2 h. With ethyl acetate and dichloroethane as the solvent, a liquid-liquid biphasic reaction system was formed due to the immiscibility of these solvents with aqueous H_2O_2. To our delight, the catalyst POSS-OIM$_8$-PW also afforded very high activities and selectivity. It is worth noting that an emulsion states emerged in these biphasic reaction system after the catalyst POSS-OIM$_8$-PW was added and stirred. Similarly, the polymeric hybrids with longer alkyl side chains also acted as very active emulsion catalysts. Therefore, we suggest that the excellent catalytic activity of POSS-OIM$_x$-PW for epoxidation of alkenes largely arises from its unique amphiphilic catalyst structure.

3.3 Insight into the catalystic behavior of POSS-IL$_x$-PW

In order to confirm the amphipathicity of these polymeric hybrid catalysts, the emulsifying property of POSS-OIM$_8$-PW in H_2O_2/cyclooctene are examined and shown in Figure 9. The catalyst tends to migrate toward the oil/aqueous interface, and metastable emulsions with droplet size of about 0.4 mm are formed after stirring. The phenomenon observed here well demonstrates the amphiphilic nature of POSS-OIM$_8$-PW, and is well consistent with that of the Pickering Interfacial Catalysis [36-37], that the amphiphilic solid catalysts distributed mainly on the surface of the emulsion droplets, allowing facile separation and recycling. In terms of the above control experiments and the image of the emulsion droplet, a possible reaction model is proposed. In the microemulsion system, the substrate, H_2O_2, and catalyst interact with each other at the interfacial membrane region of each emulsion droplet. Then the H_2O_2 in aqueous phase first reacts with PW leading to the generation of active W peroxo species, which oxidize cyclooctene to cyclohexene oxide. Presumably, the amphiphilic surface and the mesoporous structure of the catalyst allows a more efficient extractiion and mass transfer of the substrate to interact with the W peroxo active species and thus promote the catalytic epoxidation performance.

4. Conclusion

In summary, we have demonstrated the successful application of octavinyl Polyhedral oligomeric silsesquioxanes (POSS) and ionic liquids as building blocks for constructing mesostructured amphiphilic Polyoxometalates (POM)-paired ionic hybrids POSS-IL*x*-PW via free radical polymerization and ion exchange reaction. The obtained hybrids were found to be highly efficient catalysts for epoxidation of cyclooctene with H_2O_2 as the oxidant. The catalyst was recovered easily and reused for five runs without observing loss in catalytic activity. The overall superior catalytic activity, high selectivity and excellent recyclability of POSS-IL*x*-PW as a heterogeneous catalyst could be attributed to its amphiphilic surface and mesoporous structure, which allow for a rapid diffusion of the reactants into the reactive PW centers.

Acknowledgements

The authors thank the National Natural Science Foundation of China (Nos. 21206052 and 21136005), the Opening Foundation of the State Key Laboratory of Materials-Oriented Chemical Engineering (No. KL13-09), and MOE & SAFEA for the 111 Project (No. B13025).

Notes and references

[a] The Key Laboratory of Food Colloids and Biotechnology, Ministry of Education, School of Chemical and Material Engineering, Jiangnan University, Wuxi 214122, China. Fax: +86-510-85917763; Tel: +86-510-85917090; E-mail: lengyan1114@126.com.
[b] State Key Laboratory of Materials-Oriented Chemical Engineering, College of Chemistry and Chemical Engineering, Nanjing Tech University, Nanjing 210009, China.
† Electronic Supplementary Information (ESI) available: Catalyst characterizations. See DOI: 10.1039/b000000x/.

1. A. Proust, B. Matt, R. Villanneau, G. Guillemot, P. Gouzerh, G. Izzet, *Chem. Soc. Rev.* 2012, **41**, 7384-7402.
2. J. Z. Chen, H. Li, W. W. Zhu, R. Zhang, L. Guo, C. Chen, H. M. Gan, B. N. Song, Z. S. Hou, *Catalysis Communication*,. 2014, **47**, 18-21.
3. A. Mouret, L. Leclercq, A. Muhlbauer, V. N. Rataj, *Green Chem*, 2014, **16**, 269-278.
4. Z. Xi, N. Zhou, Y. Sun, K. Li, *Science*, 2001, **292**, 1139-1141.

View Article Online
DOI: 10.1039/C5NJ01541C

5. C. Zou, Z. Zhang, X. Xu, Q. Gong, J. Li, C. Wu, *J. Am. Chem. Soc*, 2012, **134**(1), 87-90.
6. G. J. Chen, Y. Zhou, P. P. Zhao, Z. Y. Long, J. Wang, *ChemPlusChem*, 2013, **78**, 561-569.
7. G. J. Chen, Y. Zhou, Z. Y. Long, X. C. Wang, J. Li, J. Wang, *ACS Appl. Mater. Interfaces*, 2014, **6**, 4438-4446.
8. Z. Y. Huo, J. Zhao, Z. W. Bu, P. T. Ma, Q. S. Liu, J. Y. Niu, J. P. Wang, *ChemCatChem*, 2014, **6**, 3096-3100.
9. V. Jallet, G. Guillemot, J. Lai, P. Bauduin, V. Nardello-Rataj, A. Proust, *Chem Commun*, 2014, **50**, 6610-6612.
10. Y. Y. Zhao, Y. Li, W. Li, Y. Q. Wu, L. X. Wu, *Langmuir*, 2010, **26**(23), 18430-18436.
11. S. Doherty, J. G. Knight, J. R. Ellison, D. Weekes, R. W. Harrington, C. Hardacre, H. Manyar, *Green Chem*, **2012**, 14, 925-929.
12. Y. Leng, J. Wang, D. R. Zhu, M. J. Zhang, P. P. Zhao, Z. Y. Long, J. Huang, *Green Chem*, 2011, **13**, 1636-1639.
13. Y. Leng, J. Wang, D. R. Zhu, X. Q. Ren, H. Q. Ge, L. Shen, *Angew. Chem*, 2009, **121**, 174-177.
14. Y. Leng, J. W. Zhao, P. P. Jiang, J. Wang, *ACS Appl. Mater. Interfaces*, 2014, **6**, 5947-5954.
15. Y. Leng, J. H. Wu, P. P. Jiang, J. Wang, *Catal Sci Technol*, 2014, **4**, 1293-1300.
16. Y. Leng, J. Liu, P. P. Jiang, J. Wang, *ACS Sustainable Chem. Eng*, 2015, **3**, 170-176.
17. S. Uchida, K. Kamata, Y. Ogasawara, M. Fujita, N. Mizuno, *Dalton Trans*, 2012, **41** (33), 9979-9983.
18. S. Wang, W. Liu, Q. Wan, Y. Liu, *Green Chem*, 2009, **11** (10), 1589-1594.
19. Q. H. Zhang, X. Huang, X. L. Wang, X. D. Jia, K. Xi, *Polymer*, 2014, **55**, 1282-1291.
20. H. B. He, B. Li, J. P. Dong, Y. Y. Lei, T. L. Wang, Q. W. Yu, Y. Q. Feng, Y. B. Sun, *ACS Appl. Mater. Inter*, 2013, **5**, 8058−8066.
21. D. Gnanasekaran, K. Madhavan, B. S. R. Reddy, *J Sci Ind Res*, 2009, **68**, 437-64.
22. K. Tanaka, Y. Chujo, *J Mater Chem*, 2012, **22**, 1733-46.
23. J. Han, Y. C. Zheng, S. Zheng, S. P. Li, T. N. Hu, A. Tang, C. Gao, *Chem Commun*, 2014, **50**, 8712-8714.
24. S. Kanehashi, Y. Tomita, K, Obokata, T. Kidesaki, S. Sato, T. Miyakoshi, K. Nagai, *Polymer*, 2013, **54**(9), 2315-2323.
25. J. Z. Li, Z. Zhou, L. Ma, G. X. Chen, Q. F. Li, *Macromolecules*, 2014, **47**, 5739-5748.
26. C. W. Chiou, Y. C. Lin, L. Wang, R. Maeda, T. Hayakawa, S. W. Kuo, *Macromolecules*, 2014, **47**(24), 8709-8721.
27. R. Goseki, A. Hirao, M. Kakimoto, T. Hayakawa, *ACS Macro Lett*, 2013, **2**, 625-629.
28. Y. Leng, J. Liu, P. Jiang, J Wang, *ACS Sustainable Chem Eng*, 2015, **3**, 170-176.
29. Y. Leng, J. Zhao, P. Jiang, J Wang, *RSC Advances*, 2015, **5**, 17709-17715.
30. B. H. Yang, J. R. Li, J. F. Wang, H. Y. Xu, S. Y. Guang, C. Li, *J Appl Pol Sci*, 2009, **111**, 2963-2969.
31. W. P. Wang, X. X. Jie, M. Fei, H. Jiang, *J Pol Res*, 2011, **18**, 13-17.
32. J. Gao, Y. Chen, B. Han, Z. Feng, C. Li, N. Zhou, S. Gao, Z. Xi, *J Mol Catal A*, 2004, **210**, 197-204.
33. S. Zhang, S. Gao, Z. Xi, J. Xu, *Catal Commun*, 2007, **8**, 531-534.
34. J. Li, S. Gao, M. Li, R. Zhang, Z. Xi, *J Mol Catal A*, 2004, **218**, 247-252.
35. Y. Sun, Z. Xi, G. Cao, *J Mol Catal A*, 2001, **166**, 219-224.
36. W. Zhou, L. Fang, Z. Fan, B. Albela, L. Bonneviot, F. De Campo, M. Pera-Titus, J. Clacens, *J Am Chem Soc*, 2014, **136**, 4869−4872.
37. H. Tan, P. Zhang, L. Wang, D. Yang, K. Zhou, *Chem Commun*, 2011, **47**, 11903–11905.

View Article Online
DOI: 10.1039/C5NJ01541C

Graphical Abstract

POSS-Derived Mesoporous Ionic Copolymer-Polyoxometalate Catalysts with Surfactant Function for Epoxidation Reactions

Jiwei Zhao[a],Yan Leng*[a], Pingping Jianj [a], Jun Wang[b], and Chenjun Zhang [a]

[a] The Key Laboratory of Food Colloids and Biotechnology, Ministry of Education, School of Chemical and Material Engineering, Jiangnan University, Wuxi 214122, China;Tel: ++86-510-85917090;

E-mail: lengyan1114@126.com

[b] State Key Laboratory of Materials-Oriented Chemical Engineering,College of Chemistry and Chemical Engineering, Nanjing Tech University, Nanjing 210009, China.

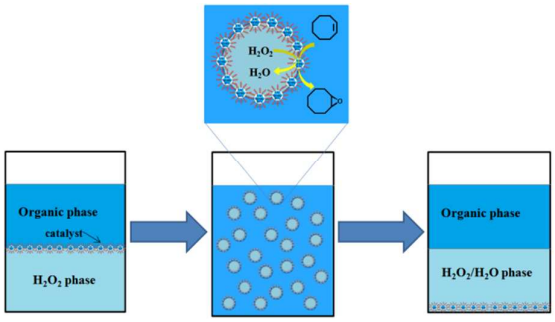

Novel Mesoporous POSS-derived POM-paired polymeric hybrids were demonstrated to be highly efficient interfacial solid catalysts for epoxidation of alkenes with H_2O_2.